WILEY | Hindawi

Research Article

The Properties of Tannery Waste Addition as a Filler Based on Two Types of Polymer Matrices: Poly(Butylene Adipate-Co-Terephthalate) (PBAT) and Poly(Butylene Succinate) (PBS)

Laksamon Raksaksri [1,2] **Yupaporn Ruksakulpiwat** [1,2] **and Thamolwan Udomkitpanya** [2]

¹*School of Polymer Engineering, Institute of Engineering, Suranaree University of Technology, Nakhon Ratchasima 30000, Thailand*
²*Research Center for Biocomposite Materials for Medical Industry and Agricultural and Food Industry, Suranaree University of Technology, Nakhon Ratchasima 30000, Thailand*

Correspondence should be addressed to Laksamon Raksaksri; laksamon@g.sut.ac.th

Wet blue leather is a waste produced by the leather industry. It is a difficult waste product to dispose of, and if not disposed of properly, it will affect the environment and cause toxicity. Therefore, recycling was considered as an alternative to waste disposal. In this study, polymer composites were prepared from two types of polymers, poly(butylene adipate-co-terephthalate) (PBAT) and poly(butylene succinate) (PBS), and wet blue leather (WBL). A twin screw extruder and injection molding were used to prepare the composites. The effect of polymer type and WBL content (5, 10, and 15 wt%) on mechanical properties, thermal properties, flammability, MFI, water absorption, and morphology was investigated. All the polymer composites showed an increase in tensile and flexural strength, Young's modulus, and water absorption but decreased in elongation at break, impact strength, and flammability compared to neat polymers.

1. Introduction

The leather industry is one of the largest in the world. Currently, approximately 1.7 billion m^2 of leather are produced worldwide with a market price of around 34 billion euros [1]. The natural properties of leather are flexibility and durability, but it has a limitation in its susceptibility to rottenness. To overcome this problem, the leather must undergo a tanning process before being used. Leather is used for different purposes including clothing (hats, jackets, skirts, trousers, and belts), footwear, bookbinding, wall covering, and furniture covering [2]. However, the tanning process is a high-emission sector which generates waste during processing. The waste consists of leftover scraps of leather cuttings produced during the manufacture of leather products [3]. About 30% of the solid waste in the tanning process consists of wet blue leather (WBL) formed by the first step of the tanning process (Figure 1) which contains chromium deriving from the chromium salts used as tanning agents [1].

Most of the tanning agents used in the tanning process are chromium (III) sulfate. The tanning agent interacts with the triple helix of the collagen, giving it leather-specific characteristics and, above all, stability [4]. However, residue management from the tanning process has become a major problem in society, especially the solid residue with potential chrome toxic effects. For years, this solid waste has been discharged into landfills or incinerated. This alternative is no longer sustainable because it involves larger environmental issues such as soil, water, and air pollution [5]. Chromium (III) used in the process can cause oxidase to toxic chromium (VI) which poses a threat to human health and the ecological environment. Hence, the way to effectively deal with WBL remains the main concern. One solution to this problem is to combine waste leather as a filler in a polymer matrix as a revolutionary alternative tannery waste management solution. Ambone et al. [6] have prepared an ecobiological composite using waste leather (WLB) as a filler in a polylactic acid (PLA) matrix as a low-cost ecofriendly

FIGURE 1: General chart of leather tanning processing.

product material. Liu et al. [4] reported on the green fabrication of leather solid waste (LSW)/thermoplastic polyurethane (TPU) composites. The LSW was prepared by a solid-state shear milling (S^3M) equipment. Xia et al. [2] have prepared cellulose/WLB composite films by a simple regeneration method. Nanni et al. [1] studied the thermomechanical and morphological properties of polymer composites reinforced with wet blue leather waste, by comparing the polymer matrices such as polyamide 12 (PA12), PLA, TPU, and thermoplastic elastomer (TPE). Ambrósio et al. [7] developed poly(vinyl butyral) (PVB)/wet blue leather fiber with leather contents of 30, 50, and 70 wt%, using a single screw extruder.

Biopolymers are widely used as substitutes for petroleum-based polymers to eliminate problems associated with both the removal of large amounts of waste and taking a long time to decompose. Therefore, more environmentally friendly biodegradable polymers are used instead [8–11] such as PLA, poly(butylene adipate-co-terephthalate) (PBAT), and poly(butylene succinate) (PBS). PBS is one of the most promising aliphatic polyesters, because it has good processability, thermal properties, and biodegradability. However, it is still limited by poor mechanical properties [10, 12, 13]. Blending with another polymer is a better solution. PBAT is a flexible aromatic aliphatic biodegradable copolyester and an ideal blending component for brittle bioplastics [8]. With the help of enzymes naturally present in fertile soil, it can fully decompose in a matter of weeks. Due to these outstanding properties, PBAT is a polymer used to replace non-biodegradable polymers in many industries such as food packaging, garbage bags, grocery bags, and agricultural film [9, 14, 15].

To enhance the properties of materials without additives, Kuang et al. [16] used a pressure-driven flow treatment for PLA toughening. With the PLA in-house preparation in the form of powders and stretching flow by compression, this postprocessing exhibited better mechanical properties and heat resistance. This method also enhanced the properties of PLA/PBAT by induced hierarchical orientation [17].

The current study aims at comparing two biodegradable polymer matrices, PBAT and PBS, incorporated with WLB contents of 5, 10, and 15 wt% using a twin screw extruder for melt mixing and injection molding for specimen preparation. The developed composites were tested for their mechanical and rheological properties, thermal stability, water absorption, and biodegradation properties to determine the possibility of using WBL with biodegradable polymers.

2. Experimental

2.1. Materials. Poly(butylene adipate-co-terephthalate) (PBAT, Ecoflex F Blend C1200) with a melt flow index of 2.7-4.9 g/10 min (190°C, 2.16 kg) was purchased from BASF Chemical Company. Poly(butylene succinate) (PBS, FZ91PM) with a melt flow index of 5 g/10 min (190°C, 2.16 kg) was purchased from PTT MCC Biochem Co., Ltd. Wet blue leather (WBL) was provided by Kongsiri Tannery Co., Ltd.

2.2. Preparation of PBAT/WBL and PBS/WBL Composites. The WBL was selected through 40 mesh sieves and dried in a hot air oven at 80°C overnight before use. Prior to the extrusion process, PBAT or PBS pellets were dried in a hot air oven at 60°C for 6 h to remove moisture. Then, the two materials were mechanically mixed in a solid state. The ratios of the PBAT/WBL and PBS/WBL were as follows: 100/0, 95/5, 90/10, and 85/15 wt% ratios. The composites were prepared by a twin screw extruder (Brabender, PL-2100, Germany) with a screw speed of 40 rpm. The temperature profiles along the extruder barrel were 130, 135, 145, 150, and 145°C. The composite pellets were dried in a hot air oven at 60°C for 6 h before use. Injection molding was carried out with an injection machine (Nissei, PS40E5ASE, Japan) with an injection temperature of 160-175°C to obtain dumbbell and bar specimens for testing.

2.3. Characterization and Testing

2.3.1. Mechanical Properties. The tensile properties of the composites were measured according to ASTM D638 using a universal testing machine (UTM, Instron, USA) with a crosshead speed of 10 mm/min, an extensometer with a gauge length of 115 cm, and a load cell of 5 kN.

The impact strength of the sample was measured according to ASTM D256 using the Izod impact testing with a pendulum impact tester (Instron, 9050 manual model, USA). A pendulum size of 2.75 J at 3.45 m/s was used for the test.

Flexural tests were performed according to ASTM D790 using a universal testing machine (UTM, Instron, USA) under the three-point bending mode with a load cell of 5 kN, a crosshead speed of 1.7 mm/min, and a support span length of 100 mm.

2.3.2. Thermal Properties. The heat deflection temperature (HDT) of the samples was determined as the temperature at which 0.25 mm bending takes place for edgewise specimens in a silicone oil bath with a load of 125 g according to ASTM D648 using a DTUL/Vicat tester (Atlas, HDV 1, USA). The samples were initially at 30°C for 5 min and then heated at a rate of 120°C/h.

Thermogravimetric analysis (TGA) measurement was performed under a nitrogen atmosphere using a thermogravimetric analyzer (Mettler Toledo, TGA/DSC1, USA). Samples at about 5-10 mg were tested from 50°C to 600°C with a heating rate of 10°C/min.

The glass transition temperature of the samples was determined by a differential scanning calorimeter (DSC) (Netzsch, DSC 3500 Sirius, Germany). Samples of about 5-10 mg were tested under a nitrogen atmosphere at a heating

TABLE 1: Mechanical properties of neat PBAT, neat PBS, PBAT/WBL composites, and PBS/WBL composites.

Sample	Tensile strength (MPa)	Young's modulus (MPa)	Elongation at break (%)	Flexural strength (MPa)	Flexural modulus (MPa)	Impact strength (kJ·m^{-2})
Neat PBAT	17.6 ± 0.7	88.3 ± 2.9	Did not break	3.4 ± 0.0	360 ± 35	Did not break
PBAT_5WBL	16.8 ± 0.2	97.7 ± 7.6	449 ± 13	3.8 ± 0.0	391 ± 75	Did not break
PBAT_10WBL	15.5 ± 0.4	131 ± 6	359 ± 5	4.9 ± 0.0	467 ± 27	Did not break
PBAT_15WBL	15.0 ± 0.1	170 ± 5	303 ± 3	6.1 ± 0.3	534 ± 50	Did not break
Neat PBS	36.7 ± 0.7	597 ± 13	57.5 ± 2.0	21.2 ± 0.1	569 ± 30	7.6 ± 0.7
PBS_5WBL	35.9 ± 0.5	684 ± 22	15.5 ± 0.1	26.2 ± 0.3	621 ± 51	6.2 ± 0.3
PBS_10WBL	34.5 ± 0.1	749 ± 3	15.5 ± 0.7	28.6 ± 3.7	743 ± 63	6.1 ± 0.5
PBS_15WBL	32.3 ± 0.1	821 ± 21	9.3 ± 0.2	29.3 ± 0.5	779 ± 31	5.5 ± 0.6

rate of 5°C/min. The samples were first heated from -50°C to 200°C, held there for 3 min to erase the thermal history, and then cooled to -50°C and reheated to 200°C. The degree of crystallinity of the samples was calculated using the following equation: [18]

$$x_c(\%) = \frac{\Delta H_m}{\Delta H_m°(1-\varnothing)} \times 100\%, \qquad (1)$$

where xc is the degree of crystallinity, ΔH_m is the melting enthalpy (J/g) of the sample, $\Delta H°$ is the enthalpy of melting for 100% crystalline with a PBAT at 114 J/g or PBS at 110.5 J/g [19, 20], and $\varnothing$ is the weight fraction of WBL in the composites.

2.3.3. Flame Resistance. UL-94 vertical burning tests were performed according to ASTM D3801 by UL 94 Chamber (Fire Testing Technology, UK). The specimens used were of dimensions 125 mm × 13 mm × 3 mm. Five specimens were subjected to two flame applications of 10 s each. The after-flame and afterglow times were measured, and the eventual cotton ignition by flaming drops was recorded.

2.3.4. Limiting Oxygen Index (LOI). The LOI of each sample was measured according to ASTM D2863 by a limiting oxygen index tester (Fire Testing Technology, UK). The specimens used were of dimensions 130 mm × 6.5 mm × 3 mm.

2.3.5. Melt Flow Index. The melt flow index (MFI) was measured at 190°C and 2.160 kg, according to ASTM D1238 using a melt flow indexer (Kayeness, D4004, USA).

2.3.6. Moisture Absorption. The samples were dried at 60°C for 12 h to remove the moisture before testing and then immersed in deionized water at room temperature to determine their water absorption within 90 days. After removing the unbound moisture on the surface, the samples were weighed on a balance scale. The water absorption rate (WAR) was calculated using the following equation:

$$WAR(\%) = \frac{M2 - M1}{M1} \times 100, \qquad (2)$$

where $M1$ and $M2$ represent the mass of the sample before immersion and after immersion (g), respectively.

2.3.7. Morphology. The morphology of the samples was studied using a scanning electron microscope (SEM) (JEOL, NeoScope JCM-5000, Japan) in a high vacuum mode at a 10 kV accelerating voltage. Samples were fractured by liquid nitrogen and sputter-coated with gold before examination with SEM.

2.3.8. Biodegradation Test. The effective microorganisms (EM) were diluted by DI water with a ratio of EM 1 L:DI water 5 L. The dumbbell-shaped and square-shaped specimens prepared from all composites were separated and immersed in EM at room temperature within 90 days. After removing and washing, the specimens were dried at 60°C for 12 h to remove the moisture. Five dumbbell-shaped or square-shaped specimens were used in tensile testing or impact testing, using the same conditions as before.

3. Results and Discussion

3.1. Mechanical Properties

3.1.1. Tensile Properties of Control and after Biodegradation Test. Control specimens of neat PBAT, neat PBS, PBAT/ WBL composites, and PBS/WBL composites reported tensile strength, elongation at break, and Young's modulus in Table 1 and Figure 2. The tensile strength values of neat PBAT and neat PBS were 17.6 and 36.7 MPa, respectively. Neat PBS showed a higher tensile strength than neat PBAT. The addition of WBL to the matrix leads to a decrease in the tensile strength of PBAT and PBS composites. This is attributed to a stress concentration and poor interaction between the matrix and WBL filler [6, 7, 14, 19]. As shown in Figure 2(e), neat PBAT had the highest elongation at break compared to the other composites due to PBAT specimens
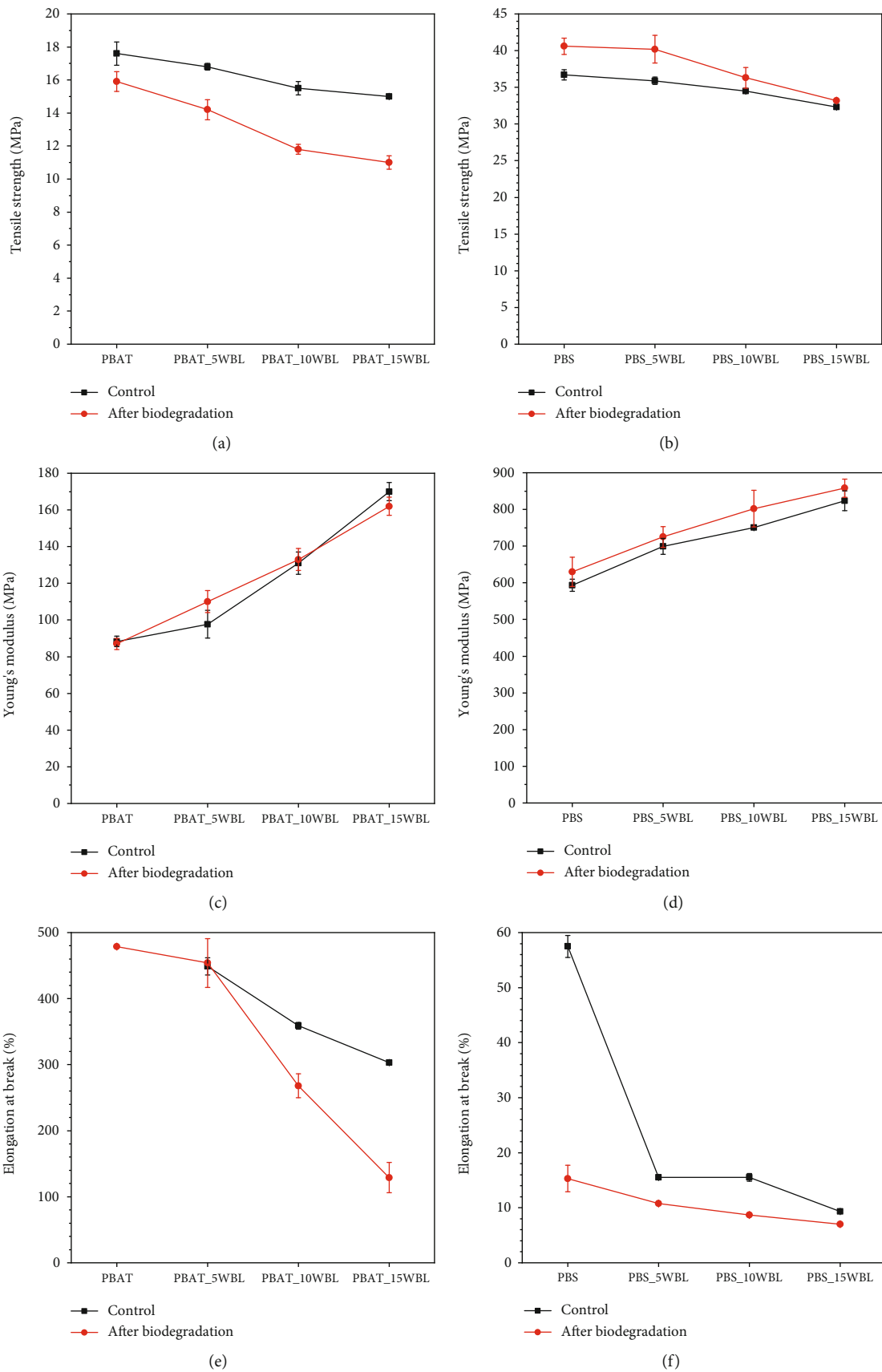
FIGURE 2: Tensile properties of control and after biodegradation test samples (a, b) tensile strength, (c, d) Young's modulus, (e, f) elongation at break.

TABLE 2: Mechanical properties of neat PBAT, neat PBS, PBAT/WBL composites, and PBS/WBL composites after the biodegradation test.

Sample	Tensile strength (MPa)	Young's modulus (MPa)	Elongation at break (%)	Impact strength (kJ·m^{-2})
Neat PBAT	15.9 ± 0.6	87 ± 3	479 ± 1	Did not break
PBAT_5WBL	14.2 ± 0.6	110 ± 6	454 ± 37	Did not break
PBAT_10WBL	11.8 ± 0.3	133 ± 6	268 ± 18	Did not break
PBAT_15WBL	11.0 ± 0.4	162 ± 5	129 ± 23	26.8 ± 0.7
Neat PBS	40.6 ± 1.1	630 ± 40	15.3 ± 2.4	3.9 ± 0.7
PBS_5WBL	40.2 ± 1.9	725 ± 28	10.8 ± 0.3	5.6 ± 0.6
PBS_10WBL	36.3 ± 1.4	802 ± 50	8.7 ± 0.1	4.5 ± 0.3
PBS_15WBL	33.2 ± 0.1	858 ± 25	7.0 ± 0.2	3.8 ± 0.2
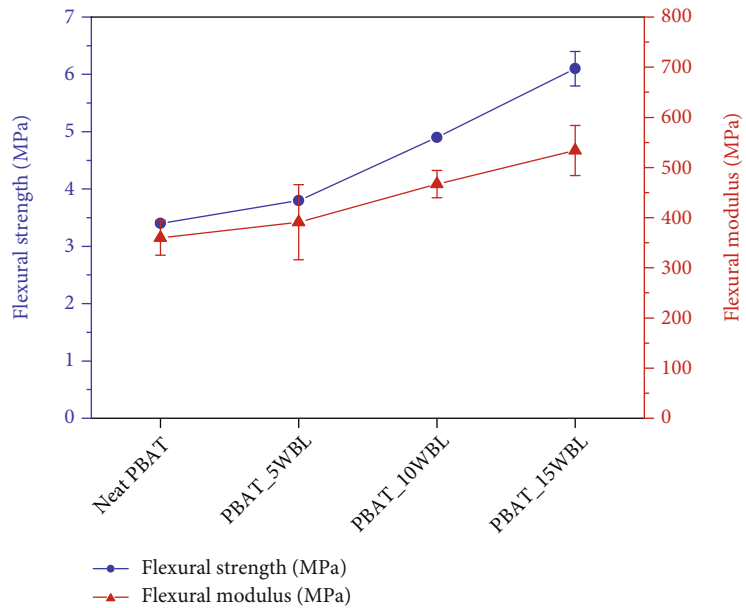
(a)
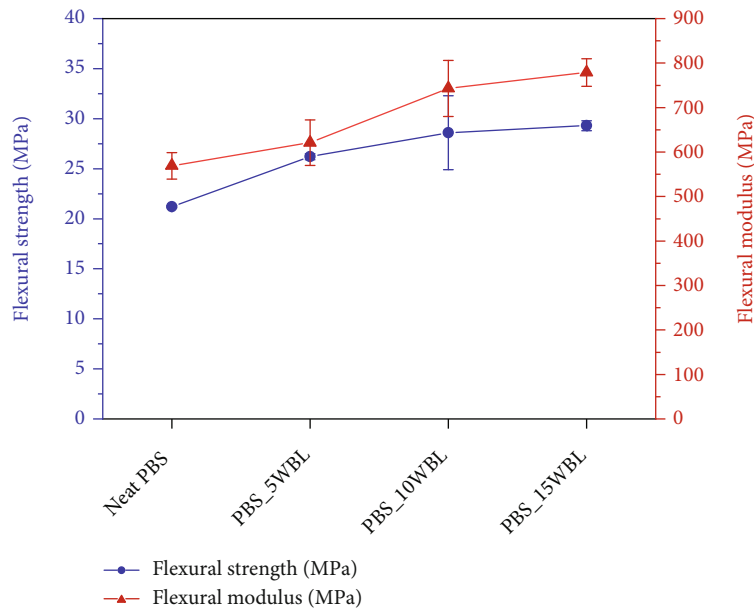
(b)

FIGURE 3: Flexural properties of (a) PBAT composites and (b) PBS composites.
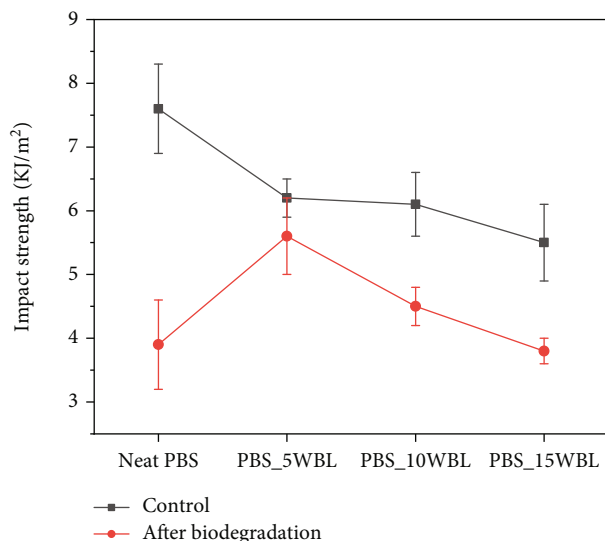
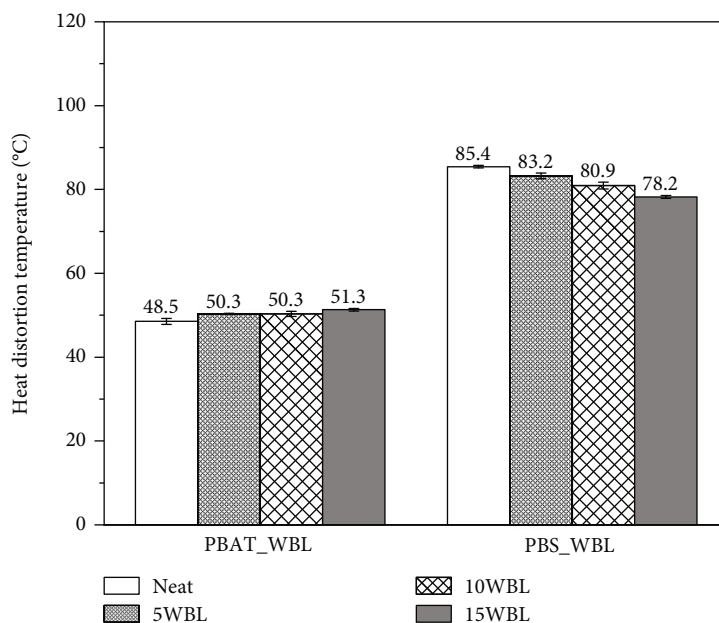FIGURE 4: Impact strength of neat PBS and PBS/WBL composites.

FIGURE 5: The heat deflection temperature of neat PBAT, neat PBS, PBAT/WBL composites, and PBS/WBL composites.

not breaking under 500% elongation. The elongation at break value of neat PBS was 57%. The elongation at break of polymer composites decreases significantly with increasing WBL content. From the results, it appears that the WBL hindered the mobility of the polymer chains leading to a reduction of the elongation at break for composites [4, 22]. On the other hand, the neat PBAT and neat PBS have shown Young's modulus of 88.3 and 63.9 MPa, respectively. The increasing WBL content leads to an increase in Young's modulus for the polymer composites because the stiffness of the WBL effectively reduces the movement within the polymer and hence enhances the rigidity of the polymer composites [7, 14, 23, 24].

The tensile properties of the neat PBAT, neat PBS, and composites after biodegradation are shown in Table 2 and illustrated in Figure 2. The tensile strength of PBAT and their composites after biodegradation in Figure 2(a) was decreased, but their Young's modulus in Figure 2(c) remains to have no significant change. In contrast, PBS and their composites after biodegradation slightly increase the tensile strength and Young's modulus as shown in Figures 2(b) and 2(d), respectively. Elongation at break of all samples after biodegradation showed the same decreasing trend. In summary, the biodegradation affected the deterioration of the biodegradable matrixes as clearly seen in the reduction of elongation at break. The increase in tensile strength and Young's modulus of neat PBS and their composites might be due to annealing during drying in the hot air oven at 60°C for 12 h after cleaning the biodegradation samples.
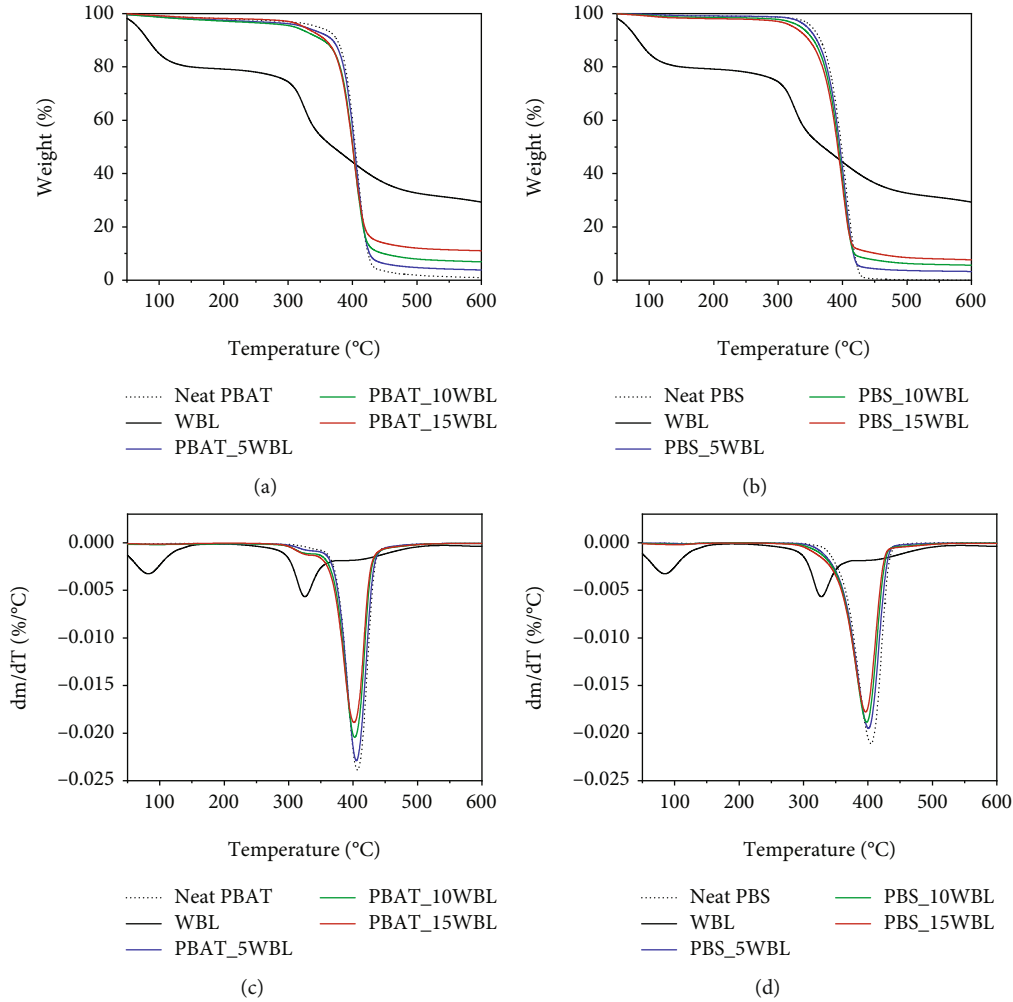
(a)

(b)

(c)

(d)

Figure 6: The TG and DTG curves of neat PBAT, neat PBS, WBL, PBAT/WBL composites, and PBS/WBL composites.

Table 3: Thermal degradation of neat PBAT, PBAT/WBL composites, neat PBS, and PBS/WBL composites.

Sample	T_o (°C)	T_d (°C)	T_e (°C)	Residue (%)
WBL	58	81	110	79.4
	304	323	371	31.3
Neat PBAT	373	404	430	2.2
PBAT_5WBL	372	402	429	4.9
PBAT_10WBL	368	400	425	7.6
PBAT_15WBL	365	399	424	12.2
Neat PBS	359	402	429	0.0
PBS_5WBL	355	398	427	4.1
PBS_10WBL	353	395	423	6.7
PBS_15WBL	351	394	421	8.3

Flexural strength represents the maximum stress exerted within a material at rupture. Figure 3 shows the flexural strength of polymer composites. The WBL enhances the flexural strength of PBAT/WBL composites and PBS/WBL composites from 3.4 to 6.1 MPa and 21.2 to 29.3 MPa, respectively, as the WBL loading is increased from 5 wt% to 15 wt%.

As a result, the addition of WBL significantly improved the flexural strength. Meanwhile, the flexural modulus of PBAT/WBL composites and PBS/WBL composites increased from 360 to 534 MPa and 569 to 779 MPa, respectively, as the loading of WBL increased from 5 wt% to 15 wt%. This is due to the high stiffness of the fibers compared to the matrices [25–27].
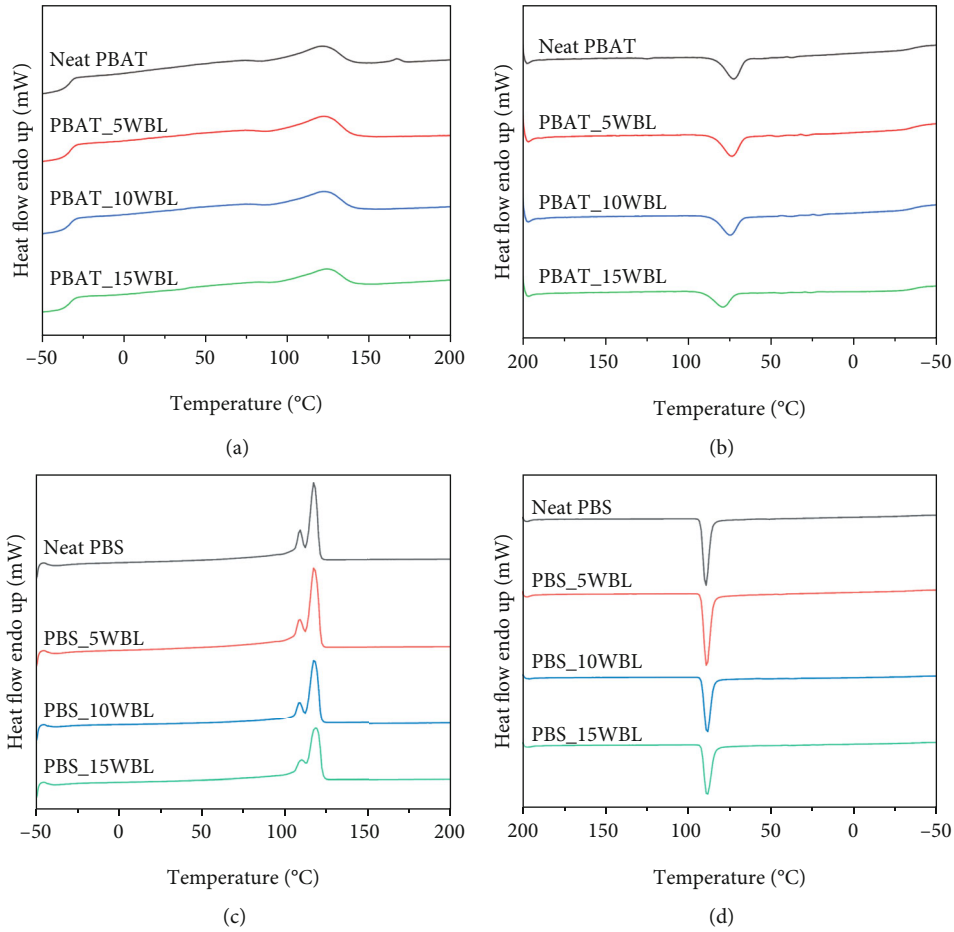
(a)

(b)

(c)

(d)

FIGURE 7: The DSC thermogram of composites: (a) the second heating of PBAT composites, (b) cooling of PBAT composites, (c) the second heating of PBS composites, and (d) cooling of PBS composites.

TABLE 4: The thermal properties of neat PBAT, PBAT/WBL composites, neat PBS, and PBS/WBL composites.

Sample	T_g (°C)	T_{m1} (°C)	ΔH_{m1} (J/g)	T_{m2} (°C)	ΔH_{m2} (J/g)	x_c (%)	T_c (°C)
Neat PBAT	−32	121	10.1	—	—	8.9	73
PBAT_5WBL	−31	122	10.9	—	—	10.1	74
PBAT_10WBL	−31	121	9.5	—	—	9.3	75
PBAT_15WBL	−31	123	7.7	—	—	7.9	80
Neat PBS	—	107	6.2	115	33.8	36.2	90
PBS_5WBL	—	106	5.0	115	38.1	41.1	90
PBS_10WBL	—	106	4.3	115	31.5	36.0	89
PBS_15WBL	—	108	2.9	116	25.7	30.4	90

This finding suggests that WBL fiber influences flexural strength. In summary, a significant increase in the flexural strength of the composites was observed.

3.1.2. Impact Strength. The Izod impact strength of control and after-degradation samples is summarized in Tables 1 and 2 and Figure 4. The impact strength of neat PBAT and PBAT/WBL composites shows no value because the samples were not broken during the impact test, which exhibited the qualities of a flexible polymer. On the other hand, the impact strength of neat PBS was 7.6 kJ·m^{-2}. WBL reduced the impact strength of PBS/WBL composites from 6.2 kJ·m^{-2} to

TABLE 5: The flame resistance properties of neat PBAT, PBAT/WBL composites, neat PBS, and PBS/WBL composites.

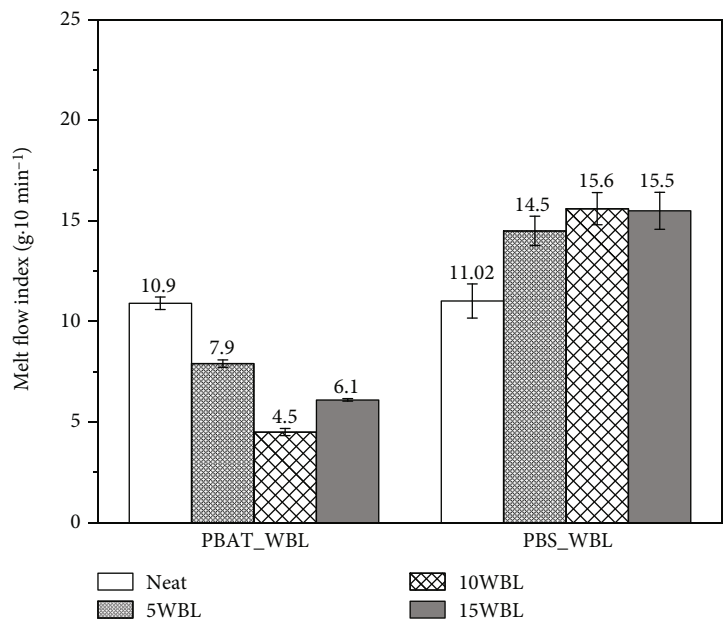| Sample	UL-94	LOI (%O2)
Neat PBAT	V-1	23.1
PBAT_5WBL	V-1	22.8
PBAT_10WBL	V-1	20.0
PBAT_15WBL	V-2	19.9
Neat PBS	V-1	24.2
PBS_5WBL	V-1	23.2
PBS_10WBL	V-1	20.0
PBS_15WBL	V-1	19.9

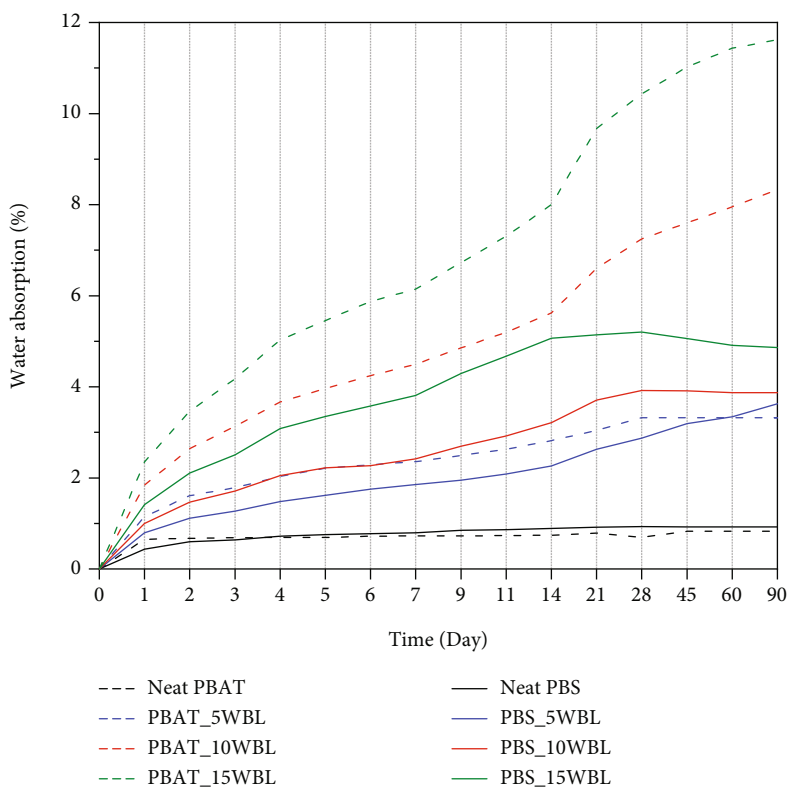FIGURE 8: Melt flow index of neat PBAT, neat PBS, PBAT/WBL composites, and PBS/WBL composites.

FIGURE 9: Water absorption of neat PBAT, neat PBS, PBAT/WBL composites, and PBS/WBL composites.

$5.5 \, \text{kJ·m}^{-2}$ as the loading of WBL increased from 5 wt% to 15 wt%. The decreasing behavior is mainly due to the inherent rigidity of WBL that physically restricts the mobility of the polymer chain and incompatibility between matrix and filler [28–31], as can be observed by SEM micrographs. After a degradation test, the impact strength of all composites tended to decrease. Even though the control PBAT_15WBL specimens did not break, they did break after biodegradation with an impact strength of $26.8 \pm 0.7 \, \text{kJ·m}^{-2}$. It can be concluded that both PBAT and PBS degrade in EM within 90 days. PBS composites showed biodegrade retardation at 5 wt% WBL based on its retention.
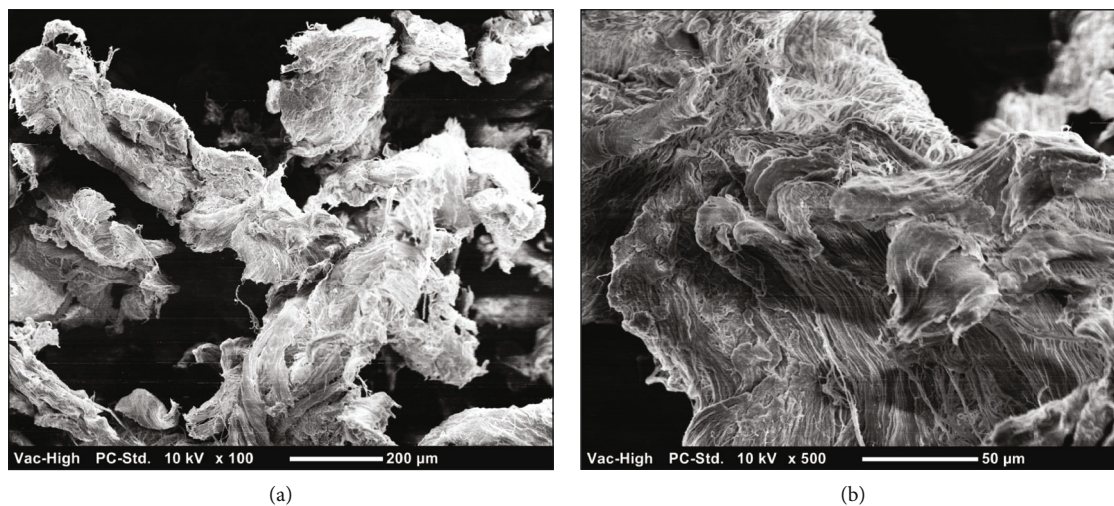
(a)

(b)

FIGURE 10: SEM micrographs of WBL (a) at 100x and (b) at 500x.
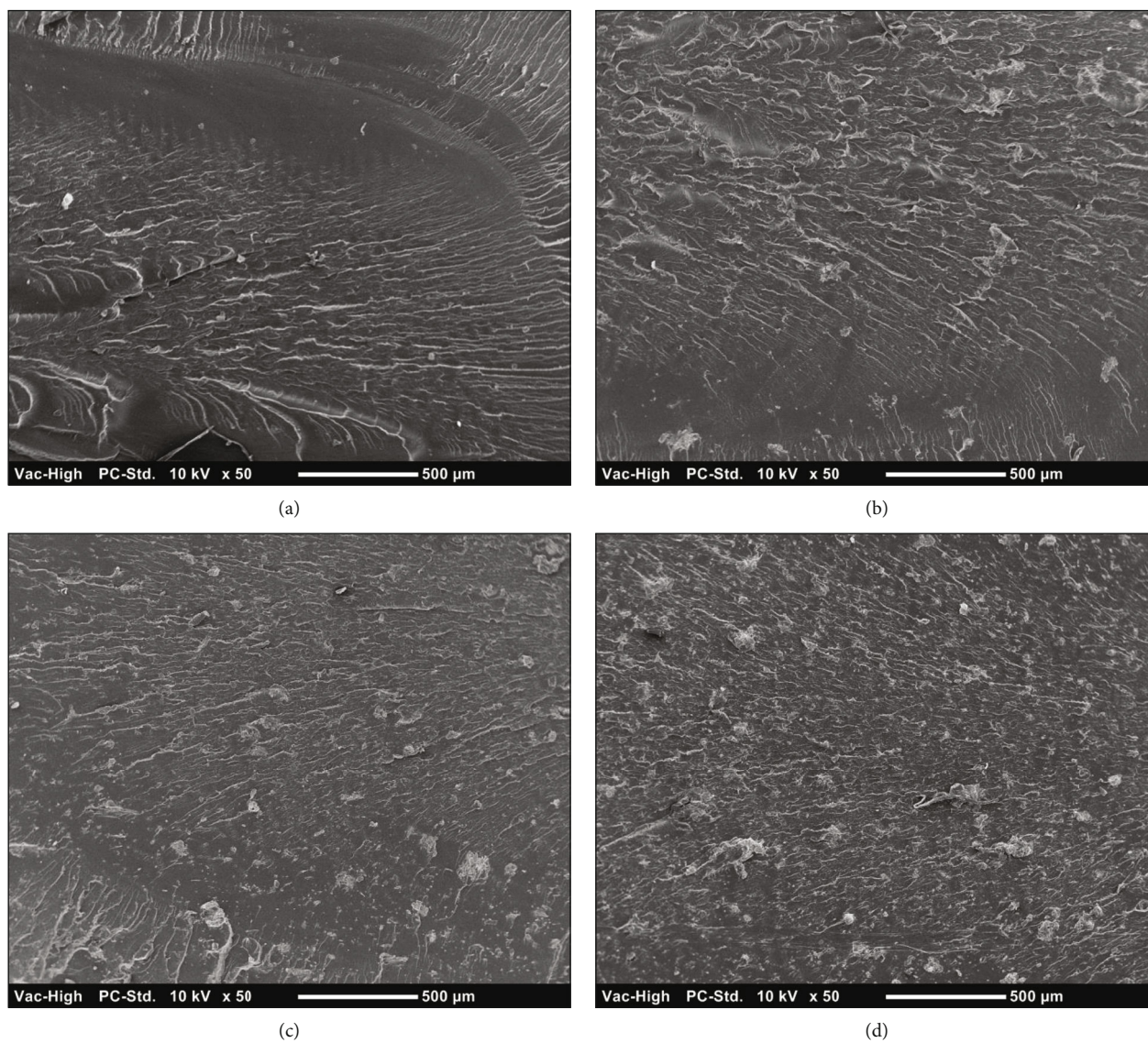

(a)

(b)

(c)

(d)

FIGURE 11: SEM micrographs (50x) of PBAT/WBL composites (a) neat PBAT, (b) PBAT_5WBL, (c) PBAT_10WBL, and (d) PBAT_15WBL.
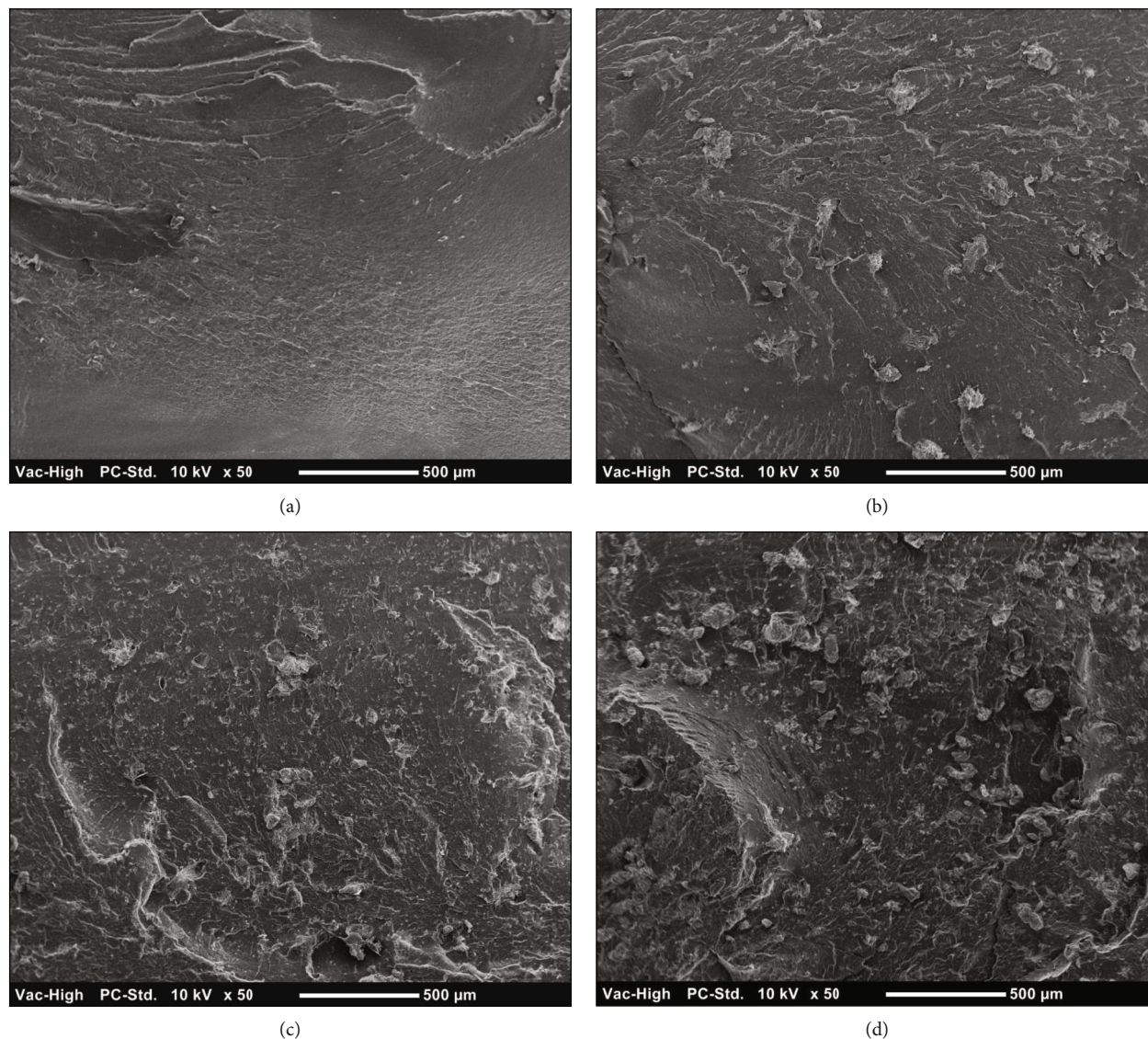
FIGURE 12: SEM micrographs (50x) of PBS/WBL composites (a) neat PBS, (b) PBS_5WBL, (c) PBS_10WBL, and (d) PBS_15WBL.

3.2. Thermal Properties

3.2.1. HDT.
The heat resistance of composites was determined by heat deflection temperature (HDT). The HDT values of the samples are presented in Figure 5. As can be seen in Figure 5, the HDT value of neat PBS was 85.4°C higher than neat PBAT which was at about 48.5°C. The HDT values of the PBS/WBL composites were slightly reduced when the WBL loading increased. The HDT value of PBS_15WBL was 78.2°C lower than neat PBS which was at about 7.2°C. Meanwhile, the HDT of the PBAT/WBL composites did not change significantly in comparison with neat PBAT. The addition of WBL from 5 wt% to 15 wt% led to HDT values changing from 48.5°C to 51.3°C. From the results, adding WBL did not increase the heat resistance of the composites.

3.2.2. TGA.
Thermal degradation and thermal stability are important parameters for polymeric materials because they can be limiting factors in processing as well as for end-of-use applications.

The TG and DTG curves of neat PBAT, PBAT/WBL composites, neat PBS, and PBS/WBL composites were investigated using thermogravimetric analysis (TGA) as shown in Figure 6. The onset temperature (T_o), decomposition temperature (T_d), endset temperature (T_e), and residue (%) of neat PBAT, neat PBS, and polymer composites are listed in Table 3. WBL shows two stages of weight loss. The first degradation stage at around 100°C was related to the dehydration of the WBL [2, 4, 7]. The main degradation stage is between 304°C and 371°C due to the weight loss in the leather's protein [2, 7]. After 371°C, the weight loss continued gradually up to 600°C. The yield residue of WBL is at about 31.3%. Meanwhile, neat PBAT, neat PBS, PBAT/WBL composites, and PBS/WBL composites show one stage of weight loss between 351°C and 430°C. The onset temperature of neat PBAT and neat PBS is 373°C and 359°C, respectively. When WBL was added, the T_o, T_d, and T_e of the polymer composites were reduced with an increasing amount of WBL. For neat PBS, no residue remained at the
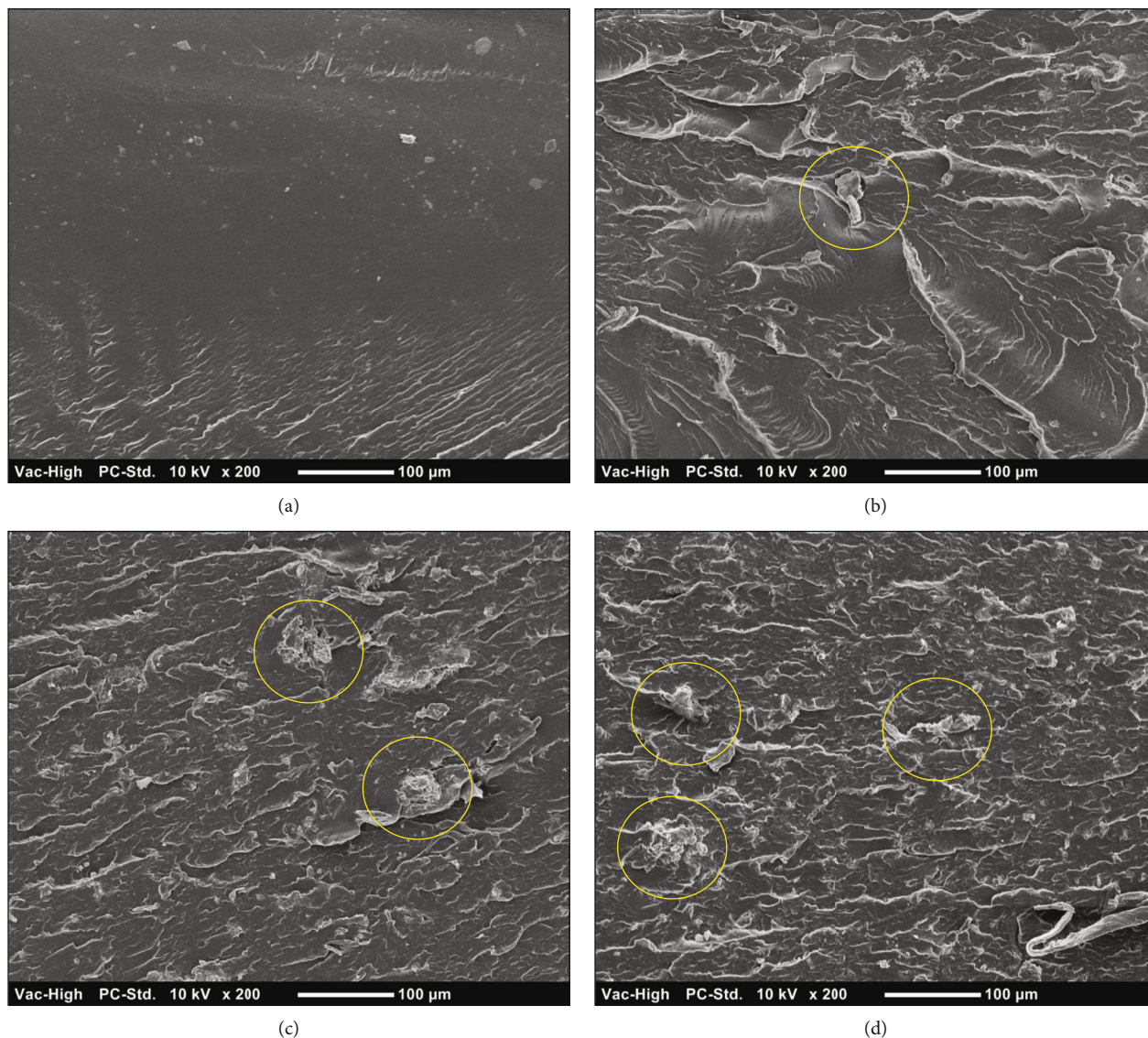
(a)

(b)

(c)

(d)

FIGURE 13: SEM micrographs (200x) of PBAT/WBL composites (a) neat PBAT, (b) PBAT_5WBL, (c) PBAT_10WBL, and (d) PBAT_15WBL.

end. From the results, the residue of polymer composites was higher than for neat polymers.

3.2.3. The Thermal Properties. The thermal properties of neat PBAT, neat PBS, PBAT/WBL composites, and PBS/WBL composites were investigated by using DSC and reported in Figure 7. The glass transition temperature (T_g), melting temperature (T_m), cooling temperature (T_c), and degree of crystallization (χ_c) are reported in Table 4. Neat PBAT gave a T_g, T_m, and T_c of -32°C, 121°C, and 73°C, respectively. The addition of WBL into PBAT did not affect T_g, T_m, and T_c. The PBAT_5WBL exhibited a degree of crystallinity of 10.1% which is higher than that of neat PBAT, indicating the ability of WBL to work as a nucleating agent for PBAT [1]. Meanwhile, adding WBL content of 10 and 15 wt% leads to a decreased degree of crystallinity of 9.3% and 7.9%, respectively, indicating that WBL impedes the crystallization of the polymer. Neat PBS gave T_{m1}, T_{m2},

and T_c of 107°C, 115°C, and 90°C, respectively. The addition of WBL into PBS led to no significant difference in T_m and T_c. The degree of crystallinity of neat PBS is 36.4%. Increasing the WBL content to 5 wt% leads to an increase in the degree of crystallinity up to 41.2%. On the other hand, PBS_10WBL and PBS_15WBL show a lower degree of crystallinity than neat PBS. The T_g of PBS does not show up in the results. Adding WBL only causes an increase in the crystallinity values.

3.3. Flammability. The LOI and UL 94 of the composites were also tested to observe the effect of WBL on the composites. Table 5 shows the LOI values and UL 94 vertical burning grades of the composites. The LOI values of the neat PBAT and neat PBS were 23.1% and 24.2%, respectively, with a V-1 rating. When WBL loading increases from 5 wt% to 15 wt%, the LOI values of the PBAT/WBL composites and PBS/WBL composites were reduced to 19.9%. The UL 94 test of PBAT_15WBL showed a reduced rating from
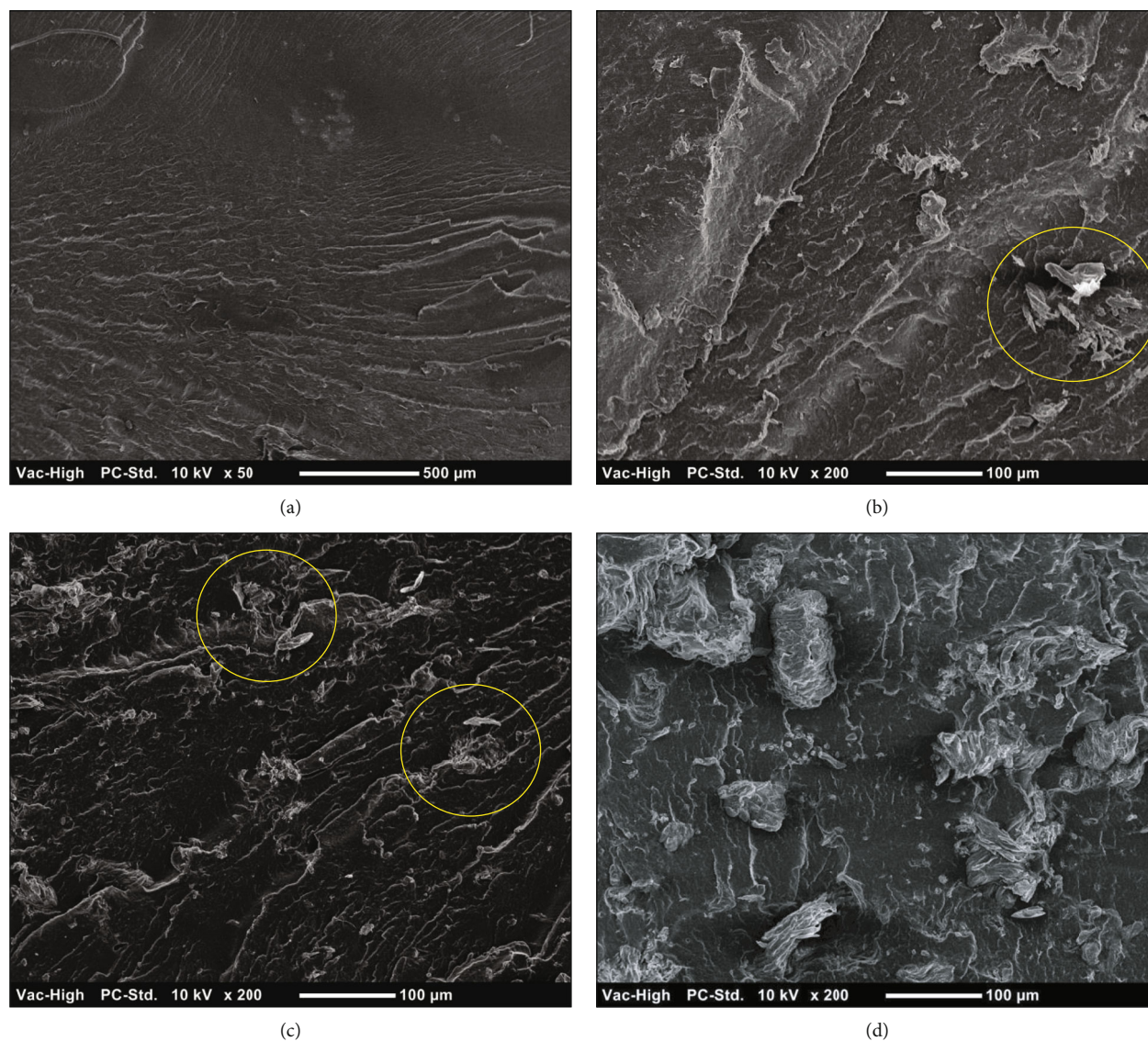
(a)

(b)

(c)

(d)

FIGURE 14: SEM micrographs (200x) of PBS/WBL composites (a) neat PBS, (b) PBS_5WBL, (c) PBS_10WBL, and (d) PBS_15WBL.

V-1 to V-2. As a result, the LOI values of all composites were approximately the same. This indicates that WBL did not improve the flame resistance of the composites.

3.4. Melt Flow Index. The MFI represents the flowability of the polymer melt under heat and pressure which indicates the viscosity of the polymer melt. The MFI of neat PBAT, neat PBS, and their composites was illustrated in Figure 8. The MFI of neat PBAT was $10.9 \, g \cdot 10 \, min^{-1}$. The addition of WBL loading from 5 wt% to 15 wt% leads to MFI values changing from $7.9 \, g \cdot 10 \, min^{-1}$ to $6.1 \, g \cdot 10 \, min^{-1}$. This indicates that the MFI decreases when adding WBL to the composites due to the fiber inherent in the mobility of the polymer chain in the melt state [32, 33], whereas the MFI value of neat PBS was $11.0 \, g \cdot 10 \, min^{-1}$. Adding WBL into the composites leads to MFI values improving from $14.5 \, g \cdot 10 \, min^{-1}$ to $15.5 \, g \cdot 10 \, min^{-1}$, while WBL loading increased from 5 wt% to 15 wt%. The MFI values

increased after adding WBL due to the lubricating effect of the fiber on the polymer chain [30].

3.5. Water Absorption. The water absorption of the composites was also tested and is shown in Figure 9. For neat PBAT and neat PBS, water was absorbed during the first stage and then reached the saturated point after 2 days. The maximum water absorption was 0.7%, indicating that the polymer matrix had no water uptake. The water absorption of PBAT with 5 wt%, 10 wt%, and 15 wt% at 90 days was 3.3%, 8.9%, and 11.4%, respectively. The water absorption of PBS with 5 wt%, 10 wt%, and 15 wt% at 90 days was 3.6%, 3.9%, and 4.7%, respectively. From the results, the maximum water absorption of PBAT/WBL composites is higher than PBS/ WBL composites. In PBAT/WBL composites and PBS/ WBL composites, an increase in water absorption with an increase in WBL content was attributed to collagen, the main structure of WBL which has hydrophilic hydroxyl

groups that allow hydrogen bond interactions with water molecules [4, 6, 27, 34, 35].

3.6. *Morphology.* Figure 10 shows micrographs of WBL where fibrous structures with various lengths and widths were observed. Higher-diameter fibers were formed by interlocking small fibers. This results in a material with flexibility and mechanical resistance.

Cryofracture surfaces on neat PBAT, neat PBS, and their composites were observed using SEM. Neat PBAT (Figure 11(a)) showed a rough surface fracture, not well defined and without a specific orientation, which exhibited characteristics of a ductile polymer. Meanwhile, the neat PBS (Figure 12(a)) showed a smooth surface fracture as a brittle polymer. The composites (Figures 11–14) had heterogeneous fracture surfaces with WBL appearing as white dots on the surface and with clearly observable phase separations. The addition of WBL loading 10 wt% and 15 wt% led to a WBL agglomerate. This is in accordance with what was observed before with tensile strength, elongation at break, and impact strength decreasing with an increasing amount of WBL. This resulted in a poor interaction between the matrix and filler with the WBL acting as a weak point in the composites. It can be concluded that shear stress during the mixing in a twin screw extruder and then injection molding was not enough to encourage interfacial adhesion between the WBL and polymer matrices.

4. Conclusion

The polymer composites with WBL loading of 5-15 wt% were successfully prepared by a twin screw extruder and then injection molding. The addition of WBL increased Young's modulus, flexural strength, flexural modulus, T_c for PBAT/WBL composites, char residue, and water absorption, especially with WBL 5 wt% acting as a nucleating agent increasing χ_c. The composites showed deterioration in tensile strength, tensile strain at break, impact strength, HDT for PBS matrix composites, T_o, T_d, T_e, and flame resistance which was mainly due to the characteristics of WBL. Melt viscosity showed variable characteristics based on their matrix. However, the fiber did not affect some results such as the HDT for PBAT matrix composites, T_g, T_m, and T_c for PBS matrix composites. After 90 days of biodegradation in EM, the tensile and impact properties decreased due to the degradation of the samples.

Data Availability

The data used to support the findings of this study are included within the supplementary information files.

Conflicts of Interest

The authors declare no conflict of interest.

Authors' Contributions

Conceptualization was contributed by L.R. and Y.R.; methodology was contributed by L.R. and T.U.; validation was contributed by L.R. and T.U.; formal analysis was contributed by T.U.; investigation was carried out by T.U.; resource was contributed by L.R.; data curation was carried out by T.U.; writing (original draft preparation) was carried out by T.U.; writing (review and editing) was carried out by L.R.; visualization was carried out by L.R.; supervision was carried out by L.R. and Y.R.; project administration was carried out by L.R. and Y.R.; funding acquisition was carried out by Y.R. and L.R. All authors have read and agreed to the published version of the manuscript.

Supplementary Materials

Table 1 raw data impact: impact strength (kJ.m^{-2}) raw data. Table 1 raw data flexural: flexural modulus (MPa) raw data. Table 2 raw data impact: impact strength (kJ.m^{-2}) after biodegradation raw data. Table 1 raw data tensile: tensile testing raw data. Figure 6 raw data HDT: heat distortion temperature raw data. Table 3 raw data: thermogravimetric analysis (TGA) raw data. Table 4 raw data: differential scanning calorimetry (DSC) raw data. Table 5 raw data UL94: UL-94 vertical burning tests raw data. Table 5 raw data LOI: limiting oxygen index tester raw data. Figure 9 raw data MFI: melt flow index raw data. Figure 10 raw data: water adsorption rate raw data. Table 2 raw data tensile: tensile testing after biodegradation raw data. (*Supplementary Materials*)

References

[1] A. Nanni, M. Parisi, M. Colonna, and M. Messori, "Thermo-mechanical and morphological properties of polymer composites reinforced by natural fibers derived from wet blue leather wastes: a comparative study," *Polymers*, vol. 13, no. 11, p. 1837, 2021.

[2] G. Xia, V. Sadanand, B. Ashok, K. O. Reddy, J. Zhang, and A. V. Rajulu, "Preparation and properties of cellulose/waste leather buff biocomposites," *International Journal of Polymer Analysis and Characterization*, vol. 20, no. 8, pp. 693–703, 2015.

[3] G. Sanchez-Olivares, A. Sanchez-Solis, F. Calderas, and J. Alongi, "Keratin fibres derived from tannery industry wastes for flame retarded PLA composites," *Polymer Degradation and Stability*, vol. 140, pp. 42–54, 2017.

[4] B. Liu, Y. Li, Q. Wang, and S. Bai, "Green fabrication of leather solid waste/thermoplastic polyurethanes composite: physically de-bundling effect of solid-state shear milling on collagen bundles," *Composites Science and Technology*, vol. 181, article 107674, 2019.

[5] M. Parisi, A. Nanni, and M. Colonna, "Recycling of chrome-tanned leather and its utilization as polymeric materials and in polymer-based composites: a review," *Polymers*, vol. 13, no. 3, article 13030429, p. 429, 2021.

[6] T. Ambone, S. Joseph, E. Deenadayalan, S. Mishra, S. Jaisankar, and P. Saravanan, "Polylactic acid (PLA) biocomposites filled with waste leather buff (WLB)," *Journal of Polymers and the Environment*, vol. 25, no. 4, pp. 1099–1109, 2017.

[7] J. D. Ambrósio, A. A. Lucas, H. Otaguro, and L. C. Costa, "Preparation and characterization of poly (vinyl butyral)-leather fiber composites," *Polymer Composites*, vol. 32, no. 5, pp. 776–785, 2011.

[8] M. Hernández-López, Z. N. Correa-Pacheco, S. Bautista-Baños et al., "Bio-based composite fibers from pine essential oil and PLA/PBAT polymer blend. Morphological, physicochemical, thermal and mechanical characterization," *Materials Chemistry and Physics.*, vol. 234, pp. 345–353, 2019.

[9] J. Jiao, X. Zeng, and X. Huang, "An overview on synthesis, properties and applications of poly(butylene-adipate-co-terephthalate)–PBAT," *Advanced Industrial and Engineering Polymer Research*, vol. 3, no. 1, pp. 19–26, 2020.

[10] S. Zhang, H. Yan, Y. Yue, and J. Guo, "Fabrication of innovative thermoplastic starch bio-elastomer to achieve high toughness poly(butylene succinate) composites," *Carbohydrate Polymers*, vol. 206, pp. 827–836, 2019.

[11] J. Zhang, V. Hirschberg, and D. Rodrigue, "Mechanical fatigue of biodegradable polymers: a study on polylactic acid (PLA), polybutylene succinate (PBS) and polybutylene adipate terephthalate (PBAT)," *International Journal of Fatigue*, vol. 159, article 106798, 2022.

[12] N. Ketata, B. Seantier, N. Guermazi, and Y. Grohens, "On the development of a green composites based on poly (lactic acid)/poly (butylene succinate) blend matrix reinforced by long flax fibers," *Materials Today: Proceedings*, vol. 52, pp. 95–103, 2022.

[13] Z. Huang, L. Qian, Q. Yin, N. Yu, T. Liu, and D. Tian, "Biodegradability studies of poly(butylene succinate) composites filled with sugarcane rind fiber," *Polymer Testing*, vol. 66, pp. 319–326, 2018.

[14] H. Kargarzadeh, A. Galeski, and A. Pawlak, "PBAT green composites: effects of kraft lignin particles on the morphological, thermal, crystalline, macro and micromechanical properties," *Polymer*, vol. 203, article 122748, 2020.

[15] T. Mukherjee, M. Czaka, N. Kao, R. K. Gupta, H. J. Choi, and S. Bhattacharya, "Dispersion study of nanofibrillated cellulose based poly(butylene adipate-co-terephthalate) composites," *Carbohydrate Polymers*, vol. 102, pp. 537–542, 2014.

[16] T. Kuang, J. Zhang, F. Chen et al., "A simple, low-cost, and green method for preparing strong, tough, and ductile poly(-lactic acid) materials with good transparency and heat resistance," *ACS Sustainable Chemistry and Engineering*, vol. 10, no. 49, pp. 16389–16398, 2022.

[17] Z. Wang, T. Liu, J. Yang et al., "Biomimetically structured poly(lactic acid)/poly(butylene-adipate-co-terephthalate) blends with ultrahigh strength and toughness for structural application," *Applied Polymer Materials*, vol. 4, no. 12, pp. 9351–9359, 2022.

[18] J. T. Yeh, C. H. Tsou, C. Y. Huang, K. N. Chen, C. S. Wu, and W. L. Chai, "Compatible and crystallization properties of poly (lactic acid)/poly (butylene adipate-co-terephthalate) blends," *Journal of Applied Polymer Science*, vol. 116, p. 680, 2009.

[19] F. Chivrac, Z. Kadlecová, E. Pollet, and L. Avérous, "Aromatic copolyester-based nano-biocomposites: elaboration, structural characterization and properties," *Journal of Polymers and the Environment*, vol. 14, no. 4, pp. 393–401, 2006.

[20] C. Erde, B. Seyda, K. Emre, C. C. Ayşe, and T. K. Gamze, "Polybutylene Succinate (PBS) – Polycaprolactone (PCL) Blends Compatibilized with Poly(ethylene oxide)-block-poly(propylene oxide)-block-poly(ethylene oxide) (PEO-PPO-PEO) Copolymer for Biomaterial Applications," *Polymer-Plastics Technology and Engineering*, vol. 53, no. 11, pp. 1178–1193, 2014.

[21] O. Kumar, A. Suresh, and J. Anbiah, "Preparation and Characterization of Leather Polymer Composites," in *20th International Conference on Composite Materials*, pp. 19–24, Copenhagen, Denmark, 2015.

[22] S. Vorawongsagul, P. Pratumpong, and C. Pechyen, "Preparation and foaming behavior of poly (lactic acid)/poly (butylene succinate)/cellulose fiber composite for hot cups packaging application," *Food Packaging and Shelf Life*, vol. 27, article 100608, 2021.

[23] R. J. Santos, D. L. S. Agostini, F. C. Cabrera, E. R. Budemberg, and A. E. Job, "Recycling leather waste: preparing and studying on the microstructure, mechanical, and rheological properties of leather waste/rubber composite," *Polymer Composites*, vol. 36, no. 12, pp. 2275–2281, 2015.

[24] I. Georgousopoulou, S. Vouyiouka, P. Dole, and C. D. Papaspyrides, "Thermo-mechanical degradation and stabilization of poly(butylene succinate)," *Polymer Degradation and Stability*, vol. 128, pp. 182–192, 2016.

[25] J. K. Oleiwi, Q. A. Hamad, and S. A. Abdulrahman, "Flexural, impact and max. shear stress properties of fibers composite for prosthetic socket," *Materials Today: Proceedings*, vol. 56, pp. 3121–3128, 2022.

[26] N. M. Kusaseh, D. M. Nuruzzaman, N. M. Ismail, Z. Hamedon, A. Azhari, and A. K. M. A. Iqbal, "Flexure and impact properties of glass fiber reinforced nylon 6-polypropylene composites," *IOP Conference Series: Materials Science and Engineering*, vol. 319, article 012045, 2018.

[27] L. Raksaksri, P. Chaiwutthinan, A. Larpkasemsuk, S. Chuayjuljit, and A. Boonmahitthisud, "Properties of wood-plastic composites based on pvc/pla/pbat ternary blend," *Journal of Metals, Materials and Minerals*, vol. 30, no. 2, p. 124, 2020.

[28] E. Kilic, Q. Tarres, M. Delgado-Aguilar, X. Espinach, I. P. P. Fullana, and R. Puig, "Leather waste to enhance mechanical performance of high-density polyethylene," *Polymers*, vol. 12, no. 9, article 12092016, p. 2016, 2020.

[29] N. Shrivastava, O. Wooi, A. Hassan, and I. Inuwa, "Mechanical and flammability properties of poly(lactic acid)/poly(butylene adipate-co-terephthalate) blends and nanocomposites: effects of compatibilizer and graphene," *Malaysian Journal of Fundamental and Applied Sciences*, vol. 14, no. 4, pp. 425–431, 2018.

[30] P. Chaiwutthinan, S. Chuayjuljit, S. Srasomsub, and A. Boonmahitthisud, "Composites of poly(lactic acid)/poly(butylene adipate-co-terephthalate) blend with wood fiber and wollastonite: physical properties, morphology, and biodegradability," *Journal of Applied Polymer Science*, vol. 136, no. 21, article 47543, 2019.

[31] J. Kim, D. Cho, and S. W. Kang, "Correlation between functional group and formation of nanoparticles in PEBAX/Ag salt/Al salt complexes for olefin separation," *Polymers*, vol. 12, no. 3, p. 667, 2020.

[32] K. Zhang, M. Misra, and A. K. Mohanty, "Toughened sustainable green composites from poly(3-hydroxybutyrate-co-3-hydroxyvalerate) based ternary blends and miscanthus biofiber," *ACS Sustainable Chemistry & Engineering*, vol. 2, no. 10, pp. 2345–2354, 2014.

[33] R. Muthuraj, M. Misra, and A. K. Mohanty, "Biodegradable biocomposites from poly(butylene adipate-co-terephthalate) and miscanthus: preparation, compatibilization, and performance evaluation," *Journal of Applied Polymer Science*, vol. 134, no. 43, p. 45448, 2017.

[34] N. Petchwattana, J. Sanetuntikul, P. Sriromreun, and B. Narupai, "Wood plastic composites prepared from biodegradable poly(butylene succinate) and Burma Padauk sawdust (*Pterocarpus macrocarpus*): water absorption kinetics and sunlight exposure investigations," *Journal of Bionic Engineering*, vol. 14, no. 4, pp. 781–790, 2017.

[35] O. Mohamed, N. El-Sayed, and A. Abdelhakim, "Preparation and characterization of polyamide-leather wastes polymer composites," *Journal of Applied Polymer Science*, vol. 118, no. 1, pp. 446–451, 2010.